



Original Article

Structural Simulation of Mg_2SiO_4 under Compression

Nguyen Hung Son*, Nguyen Hoang Anh

*Department of Computational Physics, Hanoi University of Science and Technology,
1 Dai Co Viet, Hanoi, Vietnam*

Received 08 March 2020

Revised 14 April 2020; Accepted 18 August 2020

Abstract: The microstructure in Mg_2SiO_4 glass under high compression is studied by molecular dynamic method. This work revealed the correlation between pair radial distribution functions (PRDF) of Si-Si pair and bond angle distribution (BAD) of Si-O-Si and focus on clarifying the split peak of Si-Si PRDF. Moreover, visualizing the bonds of Si-Si at different pressures show changing of Si-Si bonds with pressure. In particular, as increasing pressure, it forms corner-sharing, edge-sharing and face-sharing bond between SiO_x coordination units results in the first peak splitting of Si-Si PRDF at high pressure. The results of Si-Si's PRDF have also been analyzed and explained in detail.

Keywords: Molecular dynamic simulation, $\text{mg}_2\text{σιο}_4$, σιο_2 , hight pressure, PRDF.

1. Introduction

The two-component oxide system (MgO-SiO_2) has been investigated extensively and applied in many important high technology fields such as biomedical glass, porous ceramic membranes, refractory brick, etc. The knowledge of the microstructure of Mg_2SiO_4 and MgSiO_3 glass and melt is essential for understanding and controlling its physical and chemical properties. Therefore, MgSiO_3 and Mg_2SiO_4 have been investigated widely for several decades [1–6]. The techniques are used in experimental measurements including: X-ray diffraction, nuclear magnetic resonance (NMR), Raman spectroscopy, X-ray absorption techniques (EXAFS and XANES) and vibrational spectroscopy. The experimental method combined with simulation techniques for clearer result. Furthermore, vibrational spectroscopy (mainly Raman) has been used for structural studies of MgO-SiO_2 binary as well as in relevant system to alkaline earth oxides.

*Corresponding author.

Email address: hungson2608@gmail.com

<https://doi.org/10.25073/2588-1124/vnumap.4484>

NMR studies [7, 8], indicated that Mg-O coordination comprise of both five-fold and six-fold, in which six-fold is dominant in both MgSiO_3 and Mg_2SiO_4 systems. In works [8, 9], the neutron scatter and x-ray diffraction experiments attributed that: Si atoms have tetrahedral form SiO_4 and average distance between Si and O is of proximately 1.6-1.64 Å; Mg atoms have mean coordination number of 4.5 ± 0.1 and 5.0 ± 0.1 (exist MgO_4 and MgO_5) corresponding to MgSiO_3 and Mg_2SiO_4 glasses. The Mg-O bond distance is approximately of 2.00 Å. By using X-ray and neutron diffraction experiments combined with a reverse Monte Carlo (RMC) simulation, The authors in [9] have shown that the average coordination number of Mg in MgSiO_3 is about 4.5. However, a similar study [10] given the average coordination is about 5.1. Base on the result of diffraction and X-ray experiments, it can be interpreted that MgSiO_3 's the structure includes MgO_4 and MgO_5 polyhedra link with the silicate network via corner sharing with SiO_4 tetrahedra. Beside, RMC simulation and experimental studies in [11] have also revealed that the fraction of MgO_4 , MgO_5 , MgO_6 is approximately 68.8%, 27.8% and 3.4%, respectively. The average Mg-O bond distance in MgO_4 is shorter than other the coordination units (MgO_5 , MgO_6), MgO_4 and MgO_6 is respectively 1.924 Å and 2.1 Å. In addition, the studies [12–15] is also indicated that the silicate network in MgSiO_3 comprises Q_1, Q_2, Q_3 , among them, Q_3 is dominant (where Q_n is the SiO_4 units with n bridging oxygens (BO), O link with least two atoms Si is BO).

The simulation methods are also used extensive in investigation the local environment and the structural property of silicate glasses and make some experiments that is difficult to implement in the fact such as: researching structure of silicate and melts especial in high pressure and temperature conditions. [15]Lubicki and lasaga predicted that Mg locates at a distorted site, with the average coordination number of 4.3 Å at Mg-O distance about 2.00 Å and two more at distance 2.20 Å suitable for MD simulation result [16]that revealed that MgO_6 distorted octahedra with a Mg-O distance of 2.07 and the average coordination numbers 5.7 Å. Simulation results of melt MgSiO_3 and MgSiO_4 indicated that the coordination number of Si increases from four-fold coordination at low pressure to six-fold at higher pressure in study [17]. In the work [2], By using molecular dynamics simulation for MgSiO_3 glass at 300 K in the 0-170 GPa pressure range, the authors have shown that: the first peak position of Si-O, Mg-O, O-O, Si-Si, Mg-Si and Mg-Mg pairs are 1.63, 1.98, 2.68, 3.00, 3.19 and 2.92 respectively. The average coordination number of Si-O, Mg-O, O-O, Si-Si, Mg-Si and Mg-Mg pairs are 4.0, 4.6, 5.8, 2.1, 4.6 and 4.5, respectively. Mean coordination number of Si-O and Mg-O increase from 4.0 and 4.6 (at ambient pressure) to 6.0 and 8.0 (at 170 GPa), respectively. The mean Si-O distance increases as increasing pressure (0-40 GPa). At 40 GPa, mean Si-O bond is approximately 1.74 Å. At pressure beyond 40 GPa, the average Si-O bond decreases linearly with pressure and have the value about 1.66-1.67 Å. For Mg-O bond, the Mg-O bond length is about 2.08 Å in 0-15 GPa range and almost independent on pressure. At pressure beyond 15 GPa, the average Mg-O bond length decreases linearly with pressure and get the value of approximately 1.94-1.96 Å at 170 GPa. Besides, the authors also showed that the PRDRs of Si-O, Mg-O, O-O, Si-Si, Mg-Si and Mg-Mg depends on the pressure. Furthermore, the first peak of Si-Si pair splits into two sub-peaks at high pressure but the cause still has not been explained clearly.

In this work, we analyzed the PRDFs data, angle distribution function at high pressure and temperature condition in MgSiO_4 system. We also explained the results in detail. The changes of PRDFs affect to the structural and melt property. In addition, correlation between PRDFs and angle distribution are revealed. This correlation has been applied to explain the first peak splitting of Si-Si PRDF and the change of the other PRDFs' characteristics under compression.

2. Calculation Method

The model of Mg_2SiO_4 has been simulated by MD including of 4998 atoms (714 atoms, 2856 atoms and 1428 Mg atoms) at 600 K and the 0-100 GPa pressure range with boundary conditions for three dimensions. The Oganov potential has been used in this work shown in equation:

$$\varphi_{ij}(r_{ij}) = \frac{q_i q_j e^2}{4\pi\epsilon_o r_{ij}} + A_{ij} \exp(-B_{ij} r_{ij}) - \frac{C_{ij}}{r_{ij}^6} \quad (1)$$

Where $\varphi_{ij}(r_{ij})$ is the interatomic potential ; ϵ_o is the permittivity of free space; r_{ij} is the distance between atoms I and j; q_i and q_j are the charges of the i th and j th atoms, respectively. This potential has also been simulated in works [18–21].

Simulation program is written by C language using Verlet algorithm with MD time step of 0.47 fs. At first, the atoms are randomly put in a simulation cell. Then, the model is heated to 6000 K to assure that the initial configuration of model is removed. Next, the model is cooled down to 5000, 4000, and finally to 3500 K. After Cooling model relaxed for a long time (10^6 MD time step) in ensemble NPT (constant temperature and pressure) to produce a model at 3500 K at ambient pressure. From now, the model called M0. Next, the model is cooled to 600 K with rate of 2.5 K/ps. Subsequently, the model is compressed at different pressures (0, 5, 10, 15, 20, 25, 30, 40, 60, 80 and 100 GPa) are relaxed for 10^6 MD time steps. The structural quality is determined by averaging over 1000 configuration during the last $5 * 10^4$ MD steps.

3. Results and Discussion

3.1. Local structure

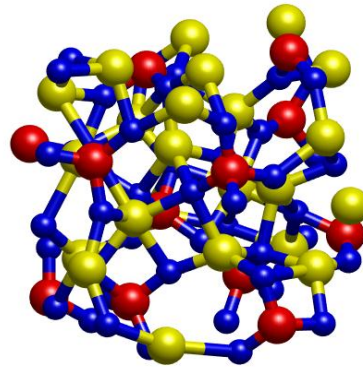


Figure 1. Network structure of Mg_2SiO_4 at ambient pressure including 12 Si atoms, 23 Mg atoms, and 43 O atoms.

Figure 1 illustrated SiO_x and MgO_x connected to each other via one common oxygen (corner-sharing) or two common oxygen (edge-sharing). At ambient pressure, the structural network only comprising SiO_4 units, and MgO_4 , MgO_5 and MgO_6 .

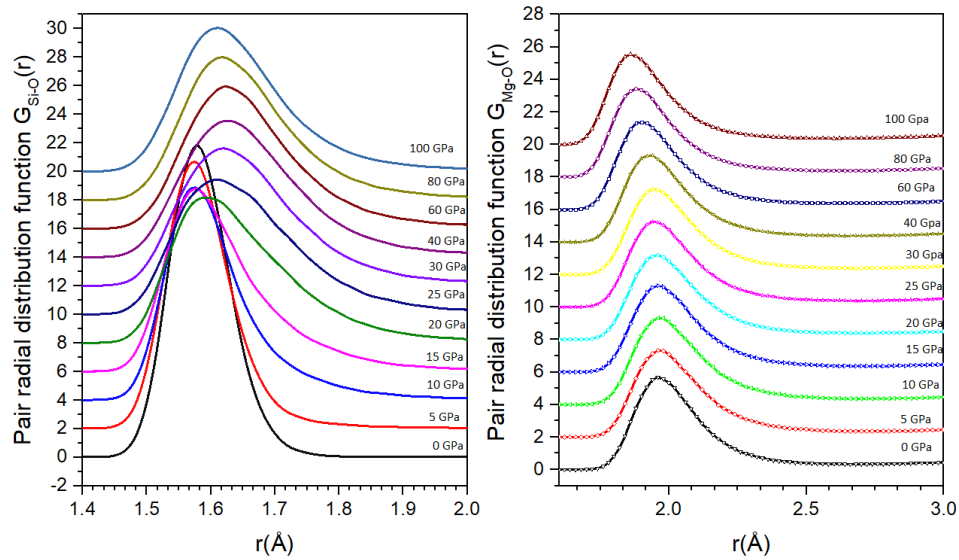


Figure 2. The PRDFs of Si-O and Mg-O pairs at different pressures.

Figure 2 shows PRDFs of Si-O and Mg-O pairs at different pressures. For Si-O, it can be seen that the position of peak is 1.58 Å at ambient pressure. Then at 0, 5, 10 and 15 GPa, the position of peak shift very slightly to the left. At higher pressure 15–40 GPa, it shifts to the right, and gets 1.66 Å at 40 GPa. At beyond 40 GPa, the first peak position moving to the left and the position of the one is 1.64 Å. For Mg-O pair, its PRDFs starting from position 2.0 Å, at ambient pressure, and it moves to the left, and its position is 1.88 at maximum pressure. The results are the same as obtaining data in works [20, 22].

Figure 3 revealed that the Si-O coordination number as a function of pressure. According to the Figure 3 the average coordination number of Si-O is approximately 4.0 at ambient pressure. It means that in the structure exists tetrahedral SiO_4 units. This is because 5- and 6-fold Si do not occur in a discrete arrangement through a corner-sharing of SiO_4 . As increasing higher pressure, the number of four-fold coordinated Si ions decreases, meanwhile the number of five- and six- fold ions increases forming SiO_5 and SiO_6 units. At 15–40 GPa, PRDFs Si-O shift to the right strongly because concentration of SiO_5 and SiO_6 units increases with pressure leading to increase the bond length. At beyond 40 GPa, the increasing SiO_6 concentration accompanied by decreasing SiO_5 , it is the reason PRDFs of Si-O is almost not change. The concentration of SiO_5 get maximum value at 30 GPa (approximately 50 %). At beyond 30 GPa, the concentration decreases with pressure. At pressure of 100 GPa, the concentration of SiO_5 is 25.3 %. For the SiO_6 , which gets value 73.5 % at pressure of 100 GPa. The average coordination number of $Si - O$ is approximately 5.20 at 30 GPa. At beyond 30 GPa, the average coordination number of Si-O increases slightly with pressure. The average coordination number of Si-O is 5.7 at 100 GPa. The results are in good agreement with experimental data as well as simulation results in work [20].

Figure 4 shows the Si-O bond angle and Si-O bond length distribution in SiO_4 , SiO_5 and SiO_6 dependent on compression. Each of these bond angle distributions $B(\theta)$ is proportional to the number of bonds between θ and $\theta + \Delta\theta$ which is dependent on the solid angle $\Delta\Omega \propto \sin(\theta)$ subtended at that value of θ [23]. The bond angle distributions are therefore plotted as $B(\theta)/\sin(\theta)$ in order to compensate for the effect of $\Delta\Omega$ such that a finite bond angle distribution at e.g. $\theta \approx 180^\circ$ is not artificially suppressed [17]. It can be seen that the O-Si-O bond angle in SiO_4 has the Gaussian form and changes slightly with

pressure. As increasing pressures, the O-Si-O BAD in SiO_4 move slightly to the left, decreasing significantly the high of peak and a little broader. In contrast, O-Si-O BAD in SiO_5 as well as SiO_6 have two peak and almost changing the location insignificantly within considered pressure ranges. The height of them are also change insignificantly with pressure ranges at nearly 90° and 170° for SiO_5 and 85° and 170° for SiO_6 . For the Si-O BLD in SiO_x where $x=4,5,6$ is also Gaussian and shift to the left as increasing pressure. The Si-O BLD in SiO_4 has the near same fraction (around 16 %) and it shifts slightly to the left as increasing pressure. At ambient pressure, Si-O BLD in SiO_4 has location of about 1.6 Å [20, 24,]. At 40 GPa pressure, the peak shift to the left to the position of 1.56-1.58 Å. At 15 GPa BLD in SiO_5 has peak at 1.64 Å. In 0-30 GPa, it shifts to the left slightly as increasing pressure. At beyond 30 GPa, it shifts stronger and the position of peak is approximately 1.58 Å at 100 GPa. Similarly, Si-O BLD in SiO_6 at pressure has a peak at 1.70 Å at 20 GPa and moving quite considerably to the left. At 100 GPa pressure, its position is at 1.64 Å. Both SiO_5 and SiO_6 have the Si-O length stabilizer with higher pressure because the peak of BLD in SiO_5 and SiO_6 units are higher at higher pressure (Figure 4).

It can be seen that the mean bond length in SiO_6 is longer than SiO_5 and the bond length in SiO_5 is longer than SiO_4 . Thus, increasing concentration of SiO_5 and SiO_6 units leads to increase of average Si-O bond length in 15-40 GPa range. In other word, the first peak of Si-O PRDF displace to the right (Figure.1). When the pressure goes up further, the bond length of SiO_5 and SiO_6 decrease due to the pressure compressing. It is the reason why the first peak of Si-O PRDF tend to move to the left at high pressure. For the Mg-O bond length, the PRDF of Mg-O (Figure 1) pair indicated that Mg-O bond length tends to decrease with pressure. Figure. 2 shows that the Mg-O coordination number increase as increasing pressure but if the Mg-O coordination number increase, the Mg-O bond length will increase due to the increase of coulomb repulsion between O^{2-} and O^{2-} ions. Therefore, this thing can be explained as following: The MgO_n (where $n=4-10$) is not stable because the Mg-O bond length distributes in a wide range and the Mg-O bond length is longer than Si-O. Hence, the affection of increasing the Mg-O coordination number is very smaller than the affection of decreasing due to compression. That the reason why the average Mg-O bond length decreases with the increase pressure.

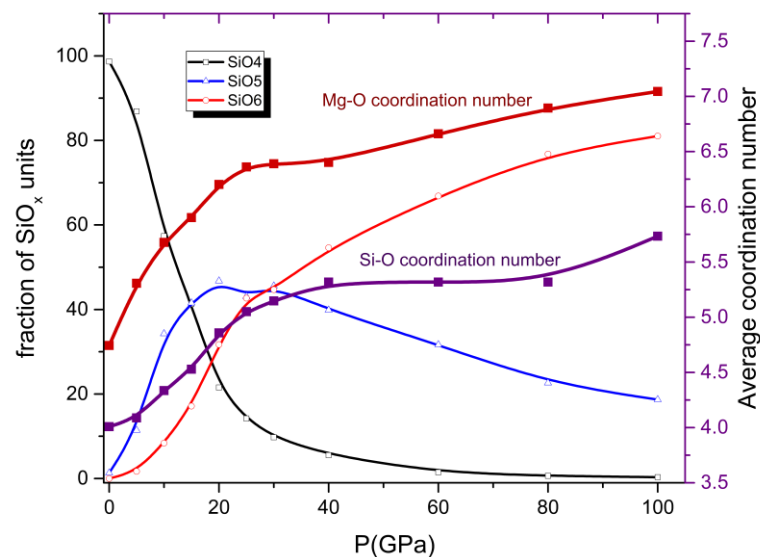


Figure 3. Si-O and Mg-O coordination number as a function of pressure.

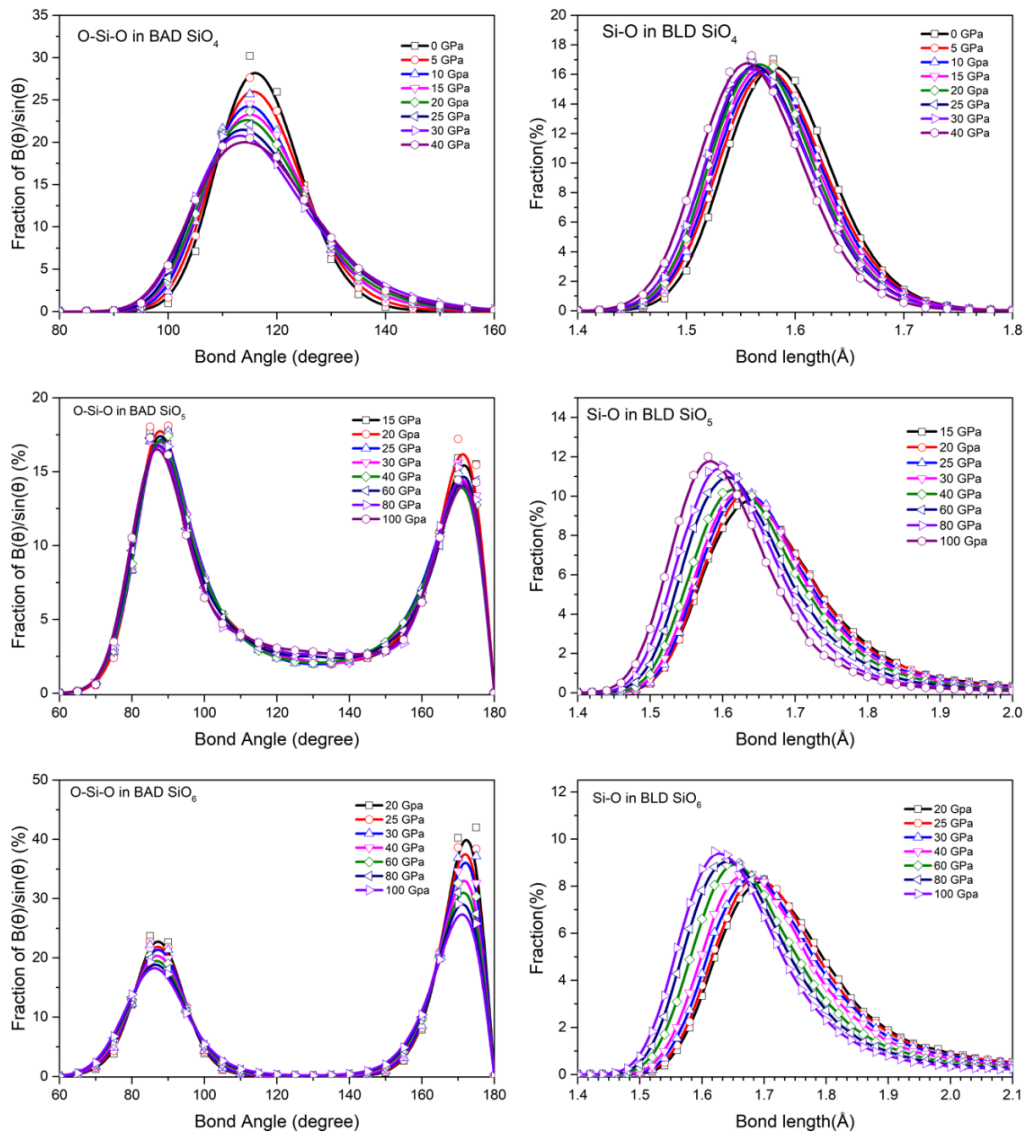


Figure 4. bond angle and bond length distribution in SiO_x ($x=4,5,6$).

3.2. Intermediate range order of Si-Si pair.

To understand the mechanism of the connection SiO_x units, we analyzed PRDFs of Si-Si pairs at different pressure (Figure 5). It can be seen that the PRDFs of Si-Si pair has a main peak at ambient pressure. In 0-20 GPa, the position of main peak is approximately of 3.00-3.10 Å, it is virtually unchanged and a little wider in considered pressure ranges. At higher pressure, existing a shoulder is on the left of the main peak and spitting a sub-peak at 40 GPa pressure. At pressure 100 GPa, the position of sub-peak is about 2.6 Å. On the right of Figure 5 shows bond angle distribution of Si-O-Si, from this data can determine the distance of Si-Si by formula:

$$d_{Si-Si} = \sqrt{d_{Si-O}^2 + d_{Si-O}^2 - 2 \cdot d_{Si-O} \cdot d_{Si-O} \cdot \cos(\widehat{Si-O-Si})}$$

here d_{Si-Si} is the Si-Si distance, d_{Si-O} is the Si-O bond length and the $\widehat{Si-O-Si}$ is the Si-O-Si bond angle. In low pressure range ($P \leq 15$ GPa) Si-O-Si BAD has a peak at around 132° , the Si-O bond length is 1.60 \AA leads to Si-Si distance is nearly $2.96\text{-}3.07 \text{ \AA}$ (the location of the main peak of Si-Si PRDF around $3.00\text{-}3.10 \text{ \AA}$). Beyond 15 GPa, there are two peaks in Si-O-Si BAD at around 97° and 133° , therefore, the calculated d_{Si-Si} is approximately 2.65 \AA and 3.10 \AA . The data results correspond with the location of the peaks on PRDFs of Si-Si pairs (Figure 5) and having good agreement with the simulation and experimental results.

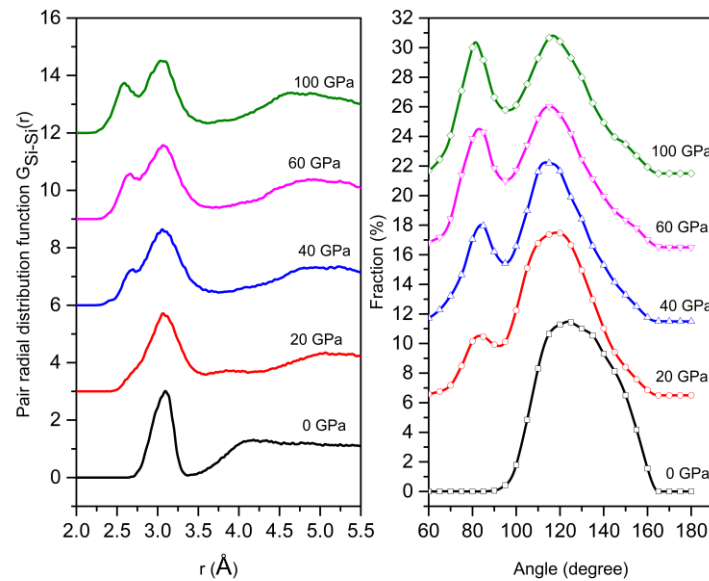


Figure 5. The Si-Si PRDF and Si-O-Si bond angle distribution at different pressures.

3.3. Visualization of silicate structure.

Table 1. distribution of corner-, edge-, and face-sharing bonds at different pressure

Pressure (GPa)	Number of different bond type			Average bond length		
	Nc	Ne	Nf	CSBL (Å)	ESBL (Å)	FSBL (Å)
0	483	0	0	3.07	NaN	NaN
5	534	2	0	3.07	2.77	NaN
10	643	20	2	3.08	2.73	2.47
15	698	43	0	3.09	2.74	NaN
20	819	81	4	3.13	2.73	2.57
25	854	123	6	3.15	2.73	2.54
30	930	138	11	3.14	2.72	2.45
40	983	158	15	3.15	2.71	2.46
60	989	254	17	3.14	2.68	2.49
80	1039	263	21	3.13	2.66	2.41
100	1045	291	26	3.11	2.63	2.42

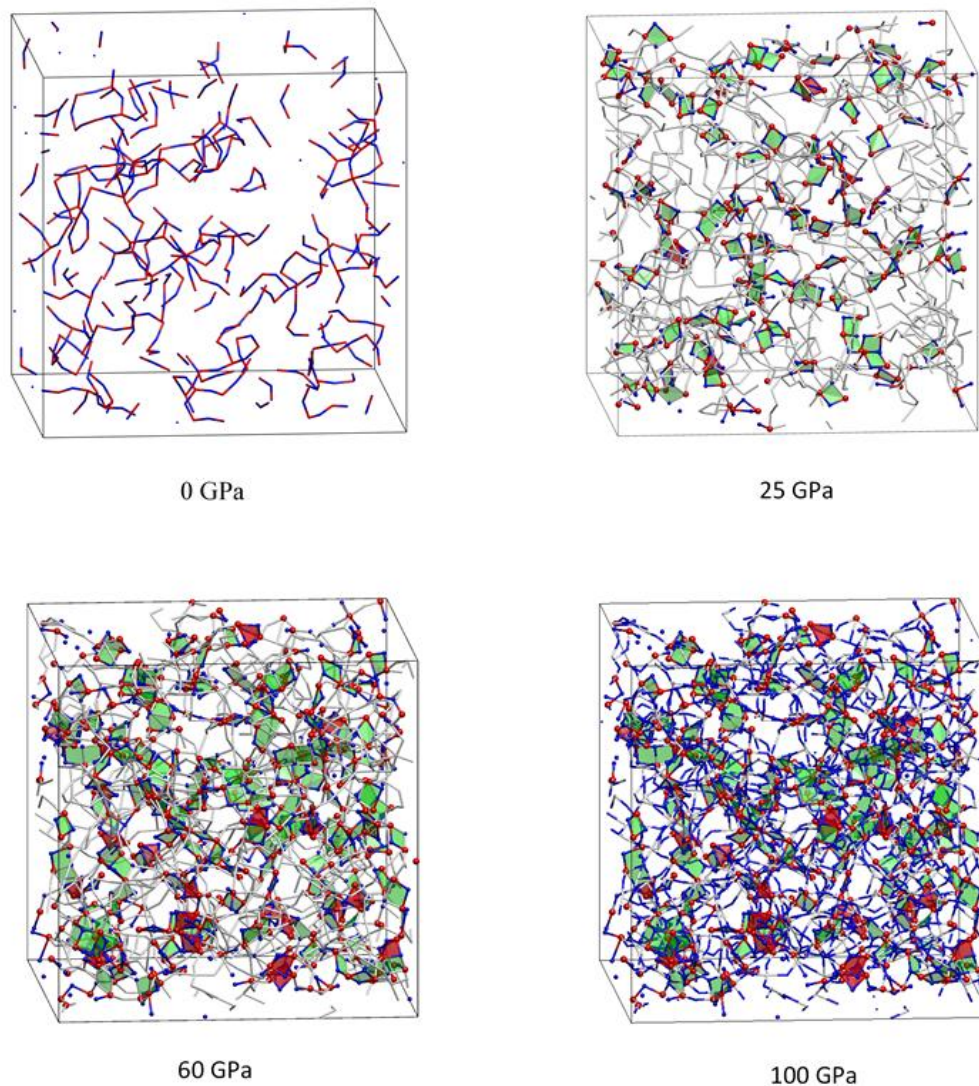


Figure 6. Visualization of corner-sharing bond (no atoms), edge-sharing-bond (green color) and face-sharing bond (red color) of SiO_x units ($x=4,5,6$).

To clarify the affection of the compression pressure to the structural changing of SiO_x units, we visualized the SiO_x 's structure (Figure. 6). At ambient pressure, the model exists 483 CSB, it can be seen that the model almost only has SiO_4 units the same as analyzing above and linked to each other through corner-sharing bond. The average bond length of corner-sharing bond oscillates from 3.07 to 3.15 Å (Table 1) corresponding the position of the first peak in Si-Si PRDF. At higher pressure (20 GPa), it includes 819 CSB, 81 ECB and 4 FCB, the corner-sharing bonds appear more numerous, at the same time, there are edge-sharing bonds also appear (ESB=81) and there are only very few face-sharing bonds (FSB=4). At 60 and 100 GPa pressure, corner-, edge-, face- sharing bonds increase significantly but corner-sharing bonds is the most (CSB=1045 at 100 GPa), so the Si-Si's PRDF is the highest and

clearest. Both CSB and ESB appear (ESB=291 and FSB=26 at 100 GPa) but only two peaks in PRDF cause by a significantly higher number of edge-sharing bond. The average of edge-sharing bond fluctuates around 2.7 Å, this value corresponds to the existence of the small shoulder at in Si-Si PRDF.

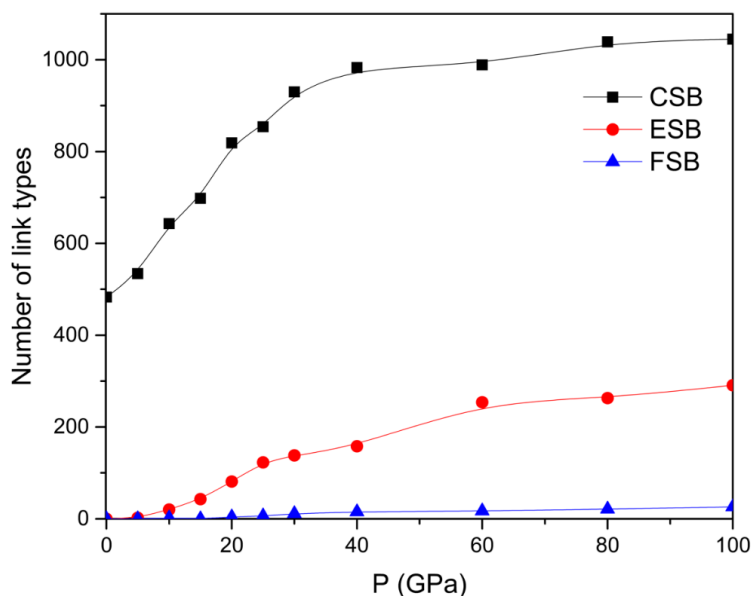


Figure 7. Number of corner-sharing bond (CSB), edge-sharing bond (ESB) and face-sharing bond (FSB) as a function of pressure.

Figure 7 indicated that the changing of number of link types (CSB, ESB and FSB) increase differently as increasing pressure. The number of Corner-sharing bonds increase strongly at 0-40 GPa, it has 483 and 983 CSB corresponding to 0 GPa and 40 GPa (Table 1). At beyond pressure, it increases slower and get 1045 CSB at 100 GPa. In contrast, the number of edge-sharing bonds rather monotonically raising is from 0 CEB at 0 GPa to 289 CEB at 100 GPa. The number of face-sharing bond also increase linear but very few, it only really exists at beyond 20 GPa and raise to 24 FSB at 100 GPa.

This is due to when rising pressure, ions are gotten closer together, leading to form bonds, this is the reason the coordination number increase under compression. The simpler structure like corner-sharing bond, it is easier to form at low pressure range. The more complex structures like edge-sharing and face-sharing bond need higher pressure to take shape.

4. Conclusion

Utilizing molecular dynamics simulation of Mg_2SiO_4 shows the changes in structural characteristics under compression. With increasing pressure, the mean Si-O coordination number gradually increases from 4 to 5.7, with five-fold and six-fold as the most abundant coordination environment eventually. The Mg-O coordination comprising of a mixture of five-, and six-fold at low pressure and peaks up more high-coordination species and its mean value increases from 4.5 to 7.5 over the entire pressure

range studied. The change of Si-O, as well as Mg-O bond length in this considered model, is clarified with pressure going up. This investigation result also reveals the tight relation between Si-Si pair radial distribution function and correspond Si-O-Si bond angle, bond length distribution. The splitting of the first peak in Si-Si pair radial distribution function and the correlation of microstructure and PRDFs characteristics are explained distinctly. Under compression, the number of linkages goes up considerably. This issue is clearly indicated in this paper and the visualization model assists to observe more easily.

Acknowledgments

The authors are grateful for support from Hanoi university of science and technology.

References

- [1] O. Glasses, Related content Densification of MgSiO₃ glass with pressure and temperature, 2010.
- [2] D.B. G, B. B. K, L. S, First-principles molecular dynamics simulations of MgSiO₃ glass : Structure , density, and elasticity at high pressure 99 (2014) 1304–1314,.
- [3] R.M. Bolis, G. Morard, T. Vinci, A. Ravasio, E. Bambrink, M. Guarguaglini, Decaying shock studies of phase transitions in MgO-SiO₂ systems : implications for the Super- Earths interiors s, 2016.
- [4] O. Adjaoud, G. Steinle-neumann, and S. Jahn, “Mg₂SiO₄ liquid under high pressure from molecular dynamics,” Chem. Geol. 256 (3–4) (2008) 184–191.
- [5] D. Der Naturwissenschaften, Mantle-Melting at High Pressure - Experimental Constraints on Magma Ocean Differentiation, 2005.
- [6] J.T.K. Wan, T.S. Duffy, S. Scandolo, R. Car, First principles study of density, viscosity, and diffusion coefficients of liquid MgSiO₃ at conditions of the Earth’s deep mantle (2005) 1–6.
- [7] S. Kohara et al., Relationship between topological order and glass forming ability in densely packed enstatite and forsterite composition glasses, Proc. Natl. Acad. Sci. U. S. A. 108, (36) (2011)14780–14785.
- [8] C.J. Benmore et al., High pressure x-ray diffraction measurements on Mg₂SiO₄ glass, J. Non. Cryst. Solids 357 (14) (2011) 2632–2636.
- [9] M.C. Wilding, C.J. Benmore, J.K.R. Weber, In situ diffraction studies of magnesium silicate liquids, J. Mater. Sci., 43(14) (2008) 4707–4713.
- [10] M. Guignard, L. Cormier, Environments of Mg and Al in MgO-Al₂O₃-SiO₂ glasses: A study coupling neutron and X-ray diffraction and Reverse Monte Carlo modeling, Chem. Geol. 256 (3–4) (2008) 111–118.
- [11] C.C. Lin, S.F. Chen, L. gun Liu, C.C. Li, Anionic structure and elasticity of Na₂O-MgO-SiO₂ glasses, J. Non. Cryst. Solids 353 (4) (2007) 413–425.
- [12] P. Zhang, P.J. Grandinetti, J.F. Stebbins, Anionic species determination in CaSiO₃ glass using two-dimensional ²⁹Si NMR, J. Phys. Chem. B. 101 (20) (1997) 4004–4008.
- [13] K.L. Sung et al., X-ray Raman scattering study of MgSiO₃ glass at high pressure: Implication for triclustered MgSiO₃ melt in Earth’s mantle, Proc. Natl. Acad. Sci. U. S. A.,105 (23) (2008) 7925–7929.
- [14] Y. Kono et al., Ultrahigh-pressure polyamorphism in GeO₂ glass with coordination number >6, Proc. Natl. Acad. Sci. U. S. A.113 (13) (2016) 3436–3441.
- [15] J.D. Kubicki, A.C. Lasaga, Molecular dynamics simulations of pressure and temperature effects on MgSiO₃ and Mg₂SiO₄ melts and glasses, Phys. Chem. Miner. 17 (8) (1991) 661–673.
- [16] K. Shimoda, M. Okuno, Molecular dynamics study of CaSiO₃-MgSiO₃ glasses under high pressure, J. Phys. Condens. Matter 18 (28) (2006) 6531–6544.
- [17] A. Zeidler et al., Structure of liquid and glassy ZnCl₂, Phys. Rev. B - Condens. Matter Mater. Phys.,82 (10) (2010) 1–17.

- [18] F.J. Spera, M.S. Ghiorso, D. Nevins, Structure, thermodynamic and transport properties of liquid MgSiO₃: Comparison of molecular models and laboratory results, *Geochim. Cosmochim. Acta* 75 (5) (2011) 1272–1296.
- [19] D. Nevins, F.J. Spera, M.S. Ghiorso, Shear viscosity and diffusion in liquid MgSiO₃: Transport properties and implications for terrestrial planet magma oceans, *Am. Mineral.*, 94 (7) (2009) 975–980.
- [20] L.T. San et al., Structural organization, micro-phase separation and polyamorphism of liquid MgSiO₃ under compression, 2016.
- [21] S.J. Gaudio, S. Sen, C.E. Lesher, Pressure-induced structural changes and densification of vitreous MgSiO₃, *Geochim. Cosmochim. Acta* 72 (4) (2008) 1222–1230.
- [22] D.B. Ghosh, B.B. Karki, First principles simulations of the stability and structure of grain boundaries in Mg₂SiO₄ forsterite, (2014) 163–171.
- [23] A. Zeidler et al., Structure of the network glass-former ZnCl₂: From the boiling point to the glass, *J. Non. Cryst. Solids* 407 (2015) 235–245.
- [24] M.C. Wilding, C.J. Benmore, J.A. Tangeman, S. Sampath, Evidence of different structures in magnesium silicate liquids: Coordination changes in forsterite- to enstatite-composition glasses, *Chem. Geol.*, 213 (1–3) (2004) 281–291.